Riginos C, Hock K, Matias AM, Mumby PJ, van Oppen MJH, Lukoschek V. 2019. **Asymmetric dispersal is a critical element of concordance between biophysical dispersal models and spatial genetic structure in Great Barrier Reef corals.** *Diversity and Distributions*
https://doi.org/10/1111/ddi.12969

Affiliations:

CR: School of Biological Sciences, The University of Queensland, St Lucia QLD, Australia; c.riginos@uq.edu.au
KH: School of Biological Sciences, The University of Queensland, St Lucia QLD, Australia; k.hock1@uq.edu.au
AMM: School of Biological Sciences, The University of Queensland, St Lucia QLD, Australia; Institute of Biology, University of the Philippines Diliman 1101, Philippines; ambrocio.matias@uqconnect.edu.au
PJM: School of Biological Sciences, The University of Queensland, St Lucia QLD, Australia; p.j.mumby@uq.edu.au
MJHvO: School of BioSciences, The University of Melbourne, VIC 3010, Australia; Australian Institute for Marine Sciences, Cape Cleveland QLD 4810, Australia; madeleine.van@unimelb.edu.au
VL: ARC Centre of Excellence for Coral Reef Studies, James Cook University, Townsville QLD 4811, Australia; vimoksalehi.lukoschek@jcu.edu.au

Abstract

Aim: Widespread coral bleaching, crown-of-thorns seastar outbreaks, and tropical storms all threaten foundational coral species of the Great Barrier Reef, with impacts differing over time and space. Yet, dispersal via larval propagules could aid reef recovery by supplying new settlers and enabling the spread of adaptive variation among regions. Documenting and predicting spatial connections arising from planktonic larval dispersal in marine species, however, remains a formidable challenge.

Location: The Great Barrier Reef, Australia

Methods: Contemporary biophysical larval dispersal models were used to predict long-distance multigenerational connections for two common and foundational coral species (*Acropora tenuis* and *Acropora millepora*). Spatially extensive genetic surveys allowed us to infer signatures of asymmetric dispersal for these species and evaluate concordance against expectations from biophysical models using coalescent genetic simulations, directions of inferred gene flow, and spatial eigenvector modelling.

Results: At long distances, biophysical models predicted a preponderance of north to south connections and genetic results matched these expectations: coalescent genetic simulations rejected an alternative scenario of historical isolation; the strongest signals of inferred gene flow were from north to south; and asymmetric eigenvectors derived from north to south connections in the biophysical models were significantly better predictors of spatial genetic patterns than eigenvectors derived from symmetric null spatial models.

Main conclusions: Results are consistent with biophysical dispersal models yielding approximate summaries of past multigenerational gene flow conditioned upon directionality of connections. For *A. tenuis* and *A. millepora,* northern and central reefs have been important sources to downstream southern reefs over the recent evolutionary past and should continue to provide southward gene flow. Endemic genetic diversity of southern reefs suggests substantial local recruitment and lack of long distance gene flow from south to north.

Key words: Approximate Bayesian Computation, asymmetric eigenvector modelling, connectivity, gene flow, marine landscape, Moran eigenvector modelling, oceanography, planktonic dispersal, seascape genetics

Introduction

Recurrent mass bleaching events on the Great Barrier Reef (GBR) have been increasing in severity and extent (Hughes et al., 2017) against a backdrop of multidecadal coral decline arising from tropical storms, crown-of-thorns seastar (COTS) predation, terrestrial runoff, and fishing pressure (De'ath, Fabricius, Sweatman, & Puotinen, 2012). Locations of severe impacts, however, differ over time. For example, northern reefs have been less affected by water quality problems and COTS outbreaks (De'ath et al., 2012), but yet the highest rates of bleaching in 2016 (the most recent and extensive mass bleaching event) were reported from these reefs (with declines of up to 60% of coral cover: Hughes et al., 2018). Within the GBR, central reefs have been most affected by terrestrial runoff, episodic COTS outbreaks (Pratchett, Caballes, Rivera-Posada, & Sweatman, 2014), tropical storms, and bleaching (De'ath et al., 2012). Southern reefs also have been subject to COTS outbreaks and tropical storms (De'ath et al., 2012), yet largely escaped bleaching in 2016 (Hughes et al., 2018).

Corals, like most benthic marine animals, have planktonic larvae potentially capable of extensive dispersal. External supplies of settlers can replenish populations; for example, following local extirpation of mature *Acropora* colonies by Cyclone Yasi, recruitment of juvenile *Acropora* was high (Lukoschek, Cross, Torda, Zimmerman, & Willis, 2013). Dispersal connections arising from planktonic larval movements can also enable the spread of adaptive variation. With temperatures and extreme heating events projected to increase in frequency (Wolff, Mumby, Devlin, & Anthony, 2018), resolving the GBR-wide capacity for adaptive gene flow (especially involving loci contributing to heat tolerance) will contribute to emerging debates regarding assisted migration and genetic rescue (Anthony et al., 2017). Of particular interest is to uncover routes of natural connections as well as pathways resistant to gene exchange.

Unfortunately, dynamics of planktonic larval dispersal over space and time remain poorly resolved (Carr et al., 2003; Kritzer & Sale, 2004) especially considering an extensive and geographically complex seascape such as the GBR. Currents and other oceanographic phenomena are inherently dynamic such that dispersal-mediated connections among populations are difficult to predict and vary by place and time (Cowen & Sponaugle, 2009; Gaggiotti, 2017; Liggins, Treml, & Riginos, 2013; Watson, Kendall, Seigel, & Mitarai, 2012). Yet, knowledge regarding the sources and destinations of dispersive larvae underpin fundamental

ecological and evolutionary dynamics and inform optimal management of marine resources for fishing and the protection of key habitats (Beger et al., 2010; Gaines, White, Carr, & Palumbi, 2010; Hock et al., 2017; Krueck et al., 2017).

Coupled biological-physical models (Cowen & Sponaugle, 2009; Werner & Cowen, 2007) relying on simulations based on species attributes and physical oceanography are increasingly being used to predict spatial and temporal aspects of planktonic larval dispersal. The flexibility of both spatio-temporal scale and outputs makes biophysical models extremely well-suited for alignment against various sources of empirical dispersal data (Cowen & Sponaugle, 2009; Jones, 2015; Kool, Moilanen, & Treml, 2013; Liggins et al., 2013) and for generating detailed spatial predictions useful for management assessments (Hock et al., 2017; as in 2016; Krueck et al., 2017).

The extent to which biophysical models accurately approximate real dispersal phenomena, however, remains an open question. As models of open natural systems, strict validation or rejection of biophysical dispersal models is not feasible (Oreskes, Shrader-Frechette, & Belitz, 1994). Rather, such models can be evaluated against empirical data whereby alignment of the model and empirical data confers increased confidence that both the model and empirically-derived statistics describe the phenomenon of interest, in this case dispersal of planktonic larvae. Geographic surveys of intraspecific genetic variation can provide important insights regarding dispersal (Hellberg, 2009; Riginos & Liggins, 2013; Selkoe et al., 2016a) and indeed several studies have considered predictions arising from biophysical dispersal models alongside observed spatial genetic patterns, typically for coastal marine taxa. Although some individual studies report correlations (Benestan et al., 2016; Dalongeville et al., 2018; Foster et al., 2012; Galindo, Olson, & Palumbi, 2006; Schunter et al., 2011; Thomas et al., 2015; Truelove et al., 2016; White et al., 2010; Xuereb et al., 2018), a recent review of the field found only moderate to low concordance between biophysical predictions and empirical genetic patterns (Selkoe, Scribner, & Galindo, 2016b).

There are many reasons why biophysical dispersal models and genetic data may not align. First, biophysical models typically focus solely on dispersal and do not consider differential recruitment and/or reproductive success of settlers (Pineda, Hare, & Sponaugle, 2007). Second, a biophysical model might not sufficiently account for important biological attributes of larvae or complex near shore oceanography, which is notoriously difficult to parameterise

120 (Metaxas & Saunders, 2009; Pineda et al., 2007; Werner & Cowen, 2007). Third, there is a
121 mismatch in time scales, where biophysical models draw upon oceanographic information
122 collected within recent years or decades whereas genetic inferences, especially those based
123 on population allele frequency differences, arise from long term processes (thousands of
124 years and longer). Fourth, population allele frequencies do not solely reflect gene flow
125 resulting from dispersal but are also shaped by changes in population sizes, range expansions,
126 colonization and so forth (Whitlock & McCauley, 1999). Lastly, although biophysical models
127 typically predict asymmetric directionality of dispersal, typical descriptors of genetic diversity
128 are symmetric so that statistical comparisons between biophysical models and empirical
129 genetic data nearly exclusively rely on transforming modelled dispersal predictions into
130 symmetric measures, greatly reducing the information content (Kool et al., 2013; Riginos,
131 Crandall, Liggins, Bongaerts, & Treml, 2016).
132
133 Only a few studies have attempted to ascertain whether empirical genetic patterns are
134 specifically consistent with the asymmetric dispersal processes inherent to biophysically
135 derived dispersal predictions. For example, migration matrices derived from biophysical
136 modelling were used to inform gene flow in forward population genetic simulations (Galindo
137 et al., 2006) and to analytically predict genetic differentiation based on forward matrix
138 projections (Kool, Paris, Andréfouët, & Cowen, 2010; Kool, Paris, Barber, & Cowen, 2011),
139 yielding outcomes that qualitatively matched empirical genetic patterns. For the Caribbean
140 coral *Orbicellea annularis*, genetic distances derived from a forward matrix project were
141 shown to be well correlated ($\rho = 0.49$) to empirical genetic distance estimates (Foster et al.,
142 2012). Another strategy draws upon historical demographic simulations to quantify
143 migration values consistent with empirically observed allele frequency spectra or DNA
144 sequences. For example, Matz *et al.* (2018) documented correlation between population
145 pairwise estimates of migration derived from allele frequency spectra against biophysically
146 derived migration probabilities for five populations for the coral *Acropora millepora* from the
147 Great Barrier Reef (GBR) (Mantel $R = 0.58$, $P = 0.05$), with a preponderance of southward
148 migration consistent between both measures. Comparing all sampled populations holistically,
149 Crandall *et al.* (2012) constructed a series of coalescent models of gene flow and contrasted
150 the likelihood of observed DNA haplotype distributions from the biophysically-informed gene
151 flow models against various other null geographic models; they demonstrated greater
152 likelihood of biophysically informed gene flow models across three species of nerite snails in

153 the South Pacific. Recently, three studies turned to asymmetric eigenvector mapping (AEM:
154 Blanchet, Legendre, Maranger, Monti, & Pepin, 2011) where asymmetric processes (such as
155 biophysical migration probabilities) are statistically modelled as spatial autocorrelation
156 structures; inclusion of AEMs substantially improved predictions of spatial genetic structure
157 for American lobster (Benestan et al., 2016), California sea cucumbers (Xuereb et al., 2018),
158 and Mediterranean striped red mullet (Dalongeville et al., 2018). Thus, these first few studies
159 that quantitatively incorporate asymmetric biophysical predictions suggest that directions of
160 larval dispersal are important elements of marine population connectivity.
161
162 Here, we comprehensively assess the alignment between biophysical models of dispersal and
163 observed spatial genetic patterns for two common broadcast spawning coral species on the
164 GBR, *Acropora tenuis* and *Acropora millepora*, drawing upon methods based on historical
165 demographic simulations, patterns of shared alleles, and AEM spatial autocorrelation
166 structures. We capitalise upon spatially rich genetic data sets for the two species (Lukoschek,
167 Riginos, & van Oppen, 2016; van Oppen, Peplow, Kinnimonth, & Berkelmans, 2011) with
168 sampling encompassing most of the 2300 km extent of the GBR. Oceanographic patterns
169 suggest that directional gene flow is likely for GBR species such as *A. tenuis* and *A. millepora*
170 (Fig. 1a).
171
172 Although present-day oceanography implies that larval dispersal can create connections
173 among distant reefs, several species show differentiation between central/northern vs.
174 southern GBR locations (reviewed by van Oppen et al., 2011), indicative of possible historical
175 vicariance associated with past sea level changes. This divergence is most notable for the
176 spiny chromis damselfish for which genetically distinct colour morphs abut at the north end
177 of Hydrographer's Channel (Planes & Doherty, 1997). Recent geological investigations,
178 however, have identified reef structures along the Australian shelf edge that may have
179 provided coral reef habitat during intermediate and low sea level stands (Abbey, Webster, &
180 Beaman, 2011; Hinestrosa, Webster, & Beaman, 2016), implying that reef species may have
181 shifted their range margins through multiple glacial cycles following the depth contours of
182 available coastline but maintaining their approximate latitudinal positions.
183
184 No single approach can simultaneously infer modern and historical gene flow regimes across
185 numerous sites spanning large spatial scales. Rather than discounting historical influences (as

is implicit in many spatial genetic methods), we use coalescent demographic simulations to evaluate competing scenarios of long-standing gene flow vs. late Quaternary divergence. The resultant affirmation of gene flow-dominated demography along the GBR justifies subsequent frequentist analyses focusing on directional gene flow inferred from population allele frequencies and using all sampled reefs. Treating the biophysical models as hypotheses of spatial connections among GBR reefs for *Acropora* corals, we test whether projected asymmetric directions and dispersal strengths are superior predictors of spatial genetic patterns as compared to simple symmetric null predictors. In addition, we examine the spatial scales and regions for which biophysical predictors best align to observed genetic patterns. This study provides a framework for aligning spatially rich population genetic data against *a priori* predictions of asymmetric dispersal and represents the most comprehensive analysis of asymmetric gene flow along the full length of the GBR to date.

METHODS

Multi-step connectivity pathways based on larval dispersal models

Connectivity modelling follows protocols described in detail by Hock et al. (in prep) with an overview in the supplementary materials. The resultant species-specific connectivity networks (based on all 3806 GBR reefs) were used to predict multistep paths between the reefs from which the genetic samples were obtained, focusing on 1) the minimum number of *stepping-stones* between two reefs (Dijkstra's 1959), 2) the *maximum flow* capacities of links necessary to connect the two nodes in a network (Ford & Fulkerson, 1956; Boykov & Kolmogorov, 2004), and 3) the *reliable path* represented by the maximum product of link weights representing the greatest chance of (direct or multi-step) larval exchange (Hock & Mumby, 2015). See supplemental methods and Sup. Fig. 1 for details and further explanation.

Genetic data

We capitalise on the extensive microsatellite datasets for *Acropora tenuis* (Lukoschek et al., 2016) and *Acropora millepora* (van Oppen et al., 2011). Some populations were merged or omitted to match the larval dispersal model, some individuals with high missing data were excluded, and conformity to Hardy-Weinberg expectations and linkage equilibria were verified. See supplemental methods.

Resolving historical influences using coalescent-based ABC

219 If allele frequencies among *Acropora* populations have been strongly influenced by past
220 interruptions to gene flow, then we would need to evaluate observed geographic
221 differentiation in light of such a divergence history. In contrast, if gene flow has dominated the
222 modern distributions of allelic diversity then dispersal interpretations based on observed
223 allele frequencies are reasonable. We used an approximate Bayesian computation (ABC)
224 approach to test the competing hypotheses of historical divergence vs. stepping-stone gene
225 flow, with the location of historical divergence set at the northern opening of Hydrographer's
226 Passage (Fig. 1). Owing to the high computational requirement in simulating genetic data to
227 match our full datasets, we used representative populations for our ABC analyses (Fig. 2). A
228 custom R script drew parameter values from the prior distributions, which were used with
229 fastSimcoal2 v2.6.0.3 (Excoffier, Dupanloup, Huerta-Sánchez, Sousa, & Foll, 2013) to generate
230 a total of 500,000 simulations, which were summarised using statistics calculated by Arlequin
231 (arlsumstat v3.5.2.2: Excoffier & Lischer, 2010). Details of simulation conditions, model
232 support, and cross-validation procedures are in the supplementary methods.
233
234 *Asymmetric gene flow and larval dispersal connectivity*
235 To estimate directionality of gene flow we use information from semi private alleles between
236 pairs of populations (Sundqvist, Keenan, Zackrisson, Prodöhl, & Kleinhans, 2016) as
237 implemented by divMigrateOnline (https://popgen.shinyapps.io/divMigrate-online/) using
238 the G_{ST} option (with no threshold for filtering out non-significant values). We assessed the
239 correlation between these asymmetric (directional) estimates of gene flow with asymmetric
240 measures of connectivity derived from the larval dispersal model (described above).
241 Significances of the correlations were evaluated using 10,000 permutations. Maximum flow
242 and reliable path metrics were (natural) log transformed for these and subsequent
243 evaluations.
244
245 *Spatial eigenvector mapping*
246 Although isolation-by-distance approaches have long been applied in spatial genetic contexts,
247 they fail to account for spatial autocorrelation structures. Moran Eigenvector Maps (MEMs)
248 model orthogonal spatial structures and, when combined with multivariate analyses, can test
249 for spatial regression (Borcard & Legendre, 2002; Dray, Legendre, & Peres-Neto, 2006) and
250 are well-suited for genetic investigations (Diniz-Filho, Nabout, Telles, Soares, & Rangel, 2009).
251 Asymmetric eigenvector maps (AEMs) extend spatial modelling to describe spatial structures

252 arising from directional processes such as ocean currents (Blanchet et al., 2011; Blanchet,
253 Legendre, & Borcard, 2008). Here we use AEMs derived from the biophysical model to test
254 whether asymmetric (directional) connectivity distances predict genetic structure, with AEM
255 model fits contrasted to null symmetric expectations described by MEMs. Creation of link
256 structures, weighting schemes, and connexion diagrams (Blanchet et al., 2008; 2011) are
257 detailed in the supplemental methods and Supp. Fig. 1. Observed population allele counts
258 were chi-square transformed (somewhat upweighting rare alleles: Legendre & Gallagher,
259 2001) to form the response variables for MEM and AEM analyses. Selection of MEM and AEM
260 model was undertaken with forward model selection based on adjusted R^2 values following
261 Dray *et al.* 2006 and Blanchet *et al.* 2011. Significance values of individual AEMs for the final
262 model were determined using redundancy analysis.
263
264 **RESULTS**
265 *Larval dispersal model*
266 Larval dispersal models for *Acropora tenuis* and *Acropora millepora* suggest that GBR
267 populations are well connected when multi-step (i.e. multigenerational) connections are
268 considered. Overall southward connections were more prevalent, especially long-distance
269 connections: this can be visualised by vectored arcs curving the right in Fig. 1B and C along
270 with greater dispersal probabilities for southwards movements (Fig. 1 D and E). However,
271 some strong northward connections were also present (vectored arcs curving the left)
272 especially among central reefs and some central to northern reefs. All three multistep
273 connectivity metrics considered were highly correlated ($\rho \geq 0.86$ for *A. tenuis*; $\rho \geq 0.80$ for *A.*
274 *millepora*) with the greatest correlations between stepping stone distance and reliable paths
275 ($\rho \geq 0.98$ for both species). Given these high correlations, we present results primarily for the
276 reliable path metric, which arguably best aligns with biological intuitions regarding
277 population connectivity across time (Hock & Mumby, 2015).
278
279 *Resolving historical influences using coalescent-based ABC*
280 In the present study, it was necessary to verify that gene flow has shaped *Acropora* spatial
281 genetic patterns and exclude vicariance as an alternative scenario before proceeding with
282 analyses that implicitly ignore divergence. Indeed, ABC analyses yielded higher support for
283 the gene flow only stepping-stone model (*A. tenuis*: posterior probability, PP= 0.999; Bayes
284 Factor, BF = 1210; *A. millepora*: PP= 0.647; BF = 3) compared to a model of historical

285 divergence vicariance. Applying model selection with the pseudo-observed data (POD)
286 yielded high accuracy (> 99 ; proportion of POD that were correctly supported) and high
287 robustness (> 99 with thresholds above 0.6 PP). Overall, these results indicate strong support
288 (sensu Roux et al., 2016) for the gene flow only stepping-stone model for both species.
289
290 *Asymmetric gene flow and larval dispersal connectivity*
291 For *A. tenuis*, all directional predictors of connectivity yielded significant correlations with
292 relative gene flow estimates from divMigrate (ρ values for stepping stone distance: -0.39;
293 maximum flow: -0.31; reliable path: -0.37; in all cases $P << 0.001$). For *A. millepora*, reliable
294 path ($\rho = -0.16$; $P < 0.005$) and stepping stone distances ($\rho = -0.13$; $P < 0.03$) were
295 significantly correlated with relative gene flow but maximum flow was not ($\rho = -0.06$; NS).
296 For both species, inspecting the relationship between reliable path probabilities and gene
297 flow (Fig. 3) shows that for populations predicted to be well connected by the larval dispersal
298 model (i.e. $P \geq 10^{-20}$) estimates of relative gene flow were highly variable (~0-1), whereas
299 sites predicted to require many stepping stone connections ($P \leq 10^{-40}$) had consistently lower
300 gene flow estimates. This pattern was stronger in *A. tenuis* than *A. millepora*.
301
302 *Spatial eigenvector mapping*
303 Directional spatial autocorrelation as assessed by AEMs explained a greater proportion of
304 variance in allele frequencies for both species (Table 1), where the best models were based on
305 alongshore north to south movements with inshore connections from the Swains to Keppel
306 Island and to the Capricorn-Bunker group (for *A. tenuis*, $R^2 = 0.37$ with 9 AEMs retained, and
307 for *A. millepora*, $R^2 = 0.27$ with 5 AEMs retained). There was no consistency in terms of best-
308 performing link weighting (i.e. stepping stone connections, maximum flow, and reliable path)
309 and notably the binary weighting (presence vs. absence, no weighting by distance) for north
310 to south connections in *A. millepora* was the best performing, indicating that simply
311 recognising strong connections (i.e. those with reliable path probabilities in the top 50th
312 percentile) yields good approximations of spatial genetic patterns. Fig. 4 depicts the highest
313 scoring AEMs for *A. tenuis* where AEM 1 (3.5% of allele frequency variance; $P = 0.001$) as the
314 largest scale of positive autocorrelation showed a gradient across the entire sampled region of
315 the GBR and AEM 5 (2.3% of variance; $P = 0.001$) described more local scale autocorrelation
316 patterns. For *A. tenuis*, AEMs 1, 5, 17, 3, 2, and 12 were individually significant at a $P = 0.05$
317 threshold based on an RDA of the final model where higher numbers (i.e. AEM17) indicate

318 finer spatial grain sizes out of a total of 19 possible AEMs of positive spatial autocorrelation.
319 For distance-based *A. tenuis* MEM models, the best model (PCNM) retained MEMs 4, 15, 35, 22
320 indicating a mix of large- and fine-scale autocorrelations. Similar results were found for *A.*
321 *millepora* (Supp Fig. 3) with AEM 1 describing the greatest amount of spatial variance in allele
322 frequencies (5.9%, P = 0.003) followed by AEM 8 (5.7%, P = 0.007), and AEMs 1, 8, 5, and 3
323 individually significant below a P = 0.05 threshold out of 9 AEMs evaluated. For distance-
324 based *A. millepora* MEM models, the best model (custom saturated) retained only MEM 12.
325 For *A. tenuis*, sampling within regions was sufficiently dense to evaluate fits for adjacent
326 regions of competing AEM models. In all instances links based on north to south alongshore
327 flow returned the best scoring models, with fit to allelic frequency patterns notably lower in
328 the far northern and northern reefs (Table 2).
329
330 **DISCUSSION**
331 Asymmetric dispersal is undoubtedly a common attribute of benthic marine species. For the
332 corals *Acropora tenuis* and *Acropora millepora*, a preponderance of north to south movement
333 along the GBR was predicted by biophysical models and this directional signal was matched in
334 patterns of microsatellite allele frequencies. Although previous studies have noted distinct
335 characteristics of northern + central vs. southern + Swains + Capricorn-Bunker regions
336 (Lukoschek et al., 2016; van Oppen et al., 2011), here we can confirm asymmetric gene flow as
337 a contributor to these regional differences. Alternative scenarios involving historical
338 divergence and symmetric gene flow were poor matches to observed spatial genetic patterns
339 relative to scenarios based on directions and extent of larval exchange predicted by
340 biophysical models. Thus, at least at the regional scale within the GBR, oceanography is likely
341 to strongly influence connections arising from planktonic larval dispersal.
342
343 *Regional connections among GBR populations*
344 Whereas geographically restricted alleles are a hallmark of long-standing isolation, highly
345 directional dispersal such as among coastal populations can result in regionally private alleles
346 in downstream populations if dispersal is sufficiently rare and when accompanied by high
347 self-recruitment of settlers to their parental populations (Pringle & Wares, 2007). This
348 expectation qualitatively matched diversity gradients for both *Acropora* species (as noted by
349 Lukoschek et al., 2016). Here, coalescent demographic simulations allowed us to formally
350 evaluate a hypothesis of Quaternary divergence against a scenario of long-standing gene flow

351 without divergence. For *A. tenuis,* we found very high support for gene flow without
352 divergence (posterior probability: 0.999; BF = 1210) and moderate support for this scenario
353 in *A. millepora* (PP= 0.647; BF = 3). Thus, if there were past divergence events, the imprint of
354 such events is no longer discernible from extant allele frequencies and present-day
355 population genetic structure should be strongly influenced by recent gene flow.
356
357 Indeed, contemporary biophysical expectations for gene flow were strong predictors of
358 genetic patterns especially at large spatial scales. Using shared alleles, the weakest genetically
359 connected population pairs (negligible gene flow from reef *i* to reef *j*) match pairs having the
360 weakest predicted multigenerational connection links (Fig. 3). Where the biophysical
361 dispersal models predicted stronger connections, in contrast, inferred gene flow was highly
362 variable indicating that at shorter distances the biophysical models and gene flow were not
363 consistently aligned. Formal statistical testing for spatial structure of allelic distributions with
364 MEMs and AEMs reinforced these findings, where eigenvectors derived from predicted
365 asymmetric connections explained considerably more variance than eigenvectors derived
366 from null geographic models of symmetric connections (Table 1). Additionally, for both *A.*
367 *tenuis* and *A. millepora* AEM 1, which describes the largest scale pattern of spatial
368 relationships (Fig. 4 and Sup. Fig. 3), explained the greatest proportion of variance in allelic
369 distributions (3.5 and 5.9% , respectively). AEM analyses, however, were also consistent with
370 spatial patterning at smaller spatial scales arising from asymmetric connections (Table 1).
371
372 That biophysical models and spatial genetic structure were misaligned at small scales does
373 not seem overly surprising. Small-scale oceanography is likely to be highly variable and may
374 lead to higher levels of mixing among local clusters of reefs than a limited number of dispersal
375 years would suggest. Moreover, the time periods are incongruent as the dispersal models
376 spanned four years (2008-2012), whereas genetic data were derived from mature colonies
377 (collected in 2009-2013 for *A. tenuis* and 2002-2009 for *A. millepora*). Additionally, chaotic
378 genetic patterns at small scales such as those observed here (Fig. 3) are well-known for
379 marine taxa, perhaps reflecting stochasticity associated with planktonic dispersal and/or
380 post-settlement selection (e.g. Johnson & Black, 1984). Finally, biophysical larval dispersal
381 models implicitly assume that post-settlement mortality rates would not be affected by
382 origins of settlers, but larval origins could influence juvenile fitness (Marshall et al. 2010).
383

384 Although spatial distributions of microsatellite alleles for both *A. tenuis* and *A. millepora* were
385 broadly consistent with asymmetric dispersal predicted by biophysical models, the best
386 alignments were obtained only considering the approximately north to south connections
387 along the length of the GBR (Table 1). Notably biophysical models for both species suggested
388 substantial counterflows (south to north) especially among inshore reefs (Fig. 1), yet adding
389 these connections to AEM models did not increase model fit (Table 1). Thus, either the
390 stronger north to south connections are sufficient for capturing most of the microsatellite
391 allelic variance or the predicted south to north movements are not realised: for example,
392 larvae may conceivably disperse northwards but could have low fitness and therefore not
393 make substantive contributions to gene flow. Matz *et al.* (2018) also detected greater
394 southwards migration among five populations of GBR *A. millepora* based on ~11,500
395 nucleotide polymorphisms, albeit with some northwards migration and only considering an
396 inshore southern reef location (Keppel Island). Southward spread also characterises Crown-
397 of-Thorns starfish outbreaks that appear to originate in northern reefs (Pratchett et al., 2014).
398 Therefore, our finding of a strong southward dispersal signal is compatible with these other
399 results, but the sensitivity of AEM based analyses to bidirectional flows is unclear.
400
401 For *A. tenuis,* we were able to further assess correlations between biophysical predictions and
402 allelic spatial distributions between adjacent regions (Table 2). For southern and central
403 reefs, north to south connections models yielded the best fits to the data ($R^2 \geq 0.32$). These
404 observations spatially align with major jets from the Coral Sea encountering the GBR and
405 driving southward advective flows along the GBR (i.e. surface waters of the South Caledonia
406 Jet at the top of the central region and Eastern Australian Current at the Swains: Choukroun,
407 Ridd, Brinkman, & McKinna, 2010; Mao & Luick, 2014). In contrast, far northern and northern
408 reefs showed reduced concordance between predictions and genetic observations ($R^2 = 0.17$)
409 with a model based on bidirectional connections yielding the best fit to this regional data;
410 surface waters of the North Caledonia Jet encounter the GBR here and creates both northward
411 and southward flows and thus might explain a possible signal of bidirectional connections
412 among *A. tenuis* populations (Choukroun et al., 2010; Mao & Luick, 2014). For both species,
413 biophysical models predict rare dispersal connections especially among far northern reefs
414 (Fig. 1) and yet negligible population structure was observed for either *A. tenuis* or *A.*
415 *millepora* among reefs in the far north (Lukoschek et al., 2016) suggesting a weaker fit
416 between dispersal models and observed genetic patterns in this region.

417

418 In summary, for the two acroporid corals considered here, we find strong support for recent
419 gene flow in a predominantly north to south direction. This result implies that northern and
420 central reefs are important sources for downstream southern reefs, at least over evolutionary
421 time scales of many generations. Southern outer shelf reef populations, however, harbour
422 greater genetic diversity than northern reefs (Lukoschek et al., 2016) and are therefore both
423 valuable in terms of distinctive diversity and, as the present results show, likely to be strongly
424 self-recruiting so that they may be more self-sustaining than central and northern reefs.
425 Dynamics of inshore reefs may be different from outer shelf reefs, for example, Lukoschek et
426 al. (2016) highlighted the genetic distinctiveness of the inshore Keppel Island population for
427 both *A. tenuis* and *A. millepora* and Matz et. al. (2018) found low genetic diversity in the
428 Keppels but with no sampling of southern outer reef populations as a basis for comparison.
429 Matz et. al. (2018) also reported low-levels of northward gene flow among their inner reef
430 populations (e.g. Keppel to Magnetic and Orpheus Islands). Further genomic studies with
431 more comprehensive spatial sampling may yield greater detailed resolution regarding rates
432 and directions of gene flow, as the microsatellite data we examined here lack the power to
433 confidently estimate specific gene flow rates.
434

435 With temperatures and extreme heating events projected to increase in frequency (Wolff et
436 al., 2018), resolving the GBR-wide capacity for gene flow including the directionality of
437 naturally occurring gene flow provides information relevant to discussions regarding assisted
438 migration and genetic rescue (Anthony et al., 2017). For example, although the southern outer
439 reefs, especially the Swains, have been largely spared from bleaching events, our results
440 indicate that naturally occurring dispersal from south to north is most likely ecologically
441 insignificant (Fig. 3), and thus would indicate that prospective migrants from the southern
442 regions would be unlikely to recolonise central and northern reefs in sufficient quantities over
443 decadal time scales. Because naturally occurring genetic rescue relies on evolutionarily
444 significant (and not ecologically significant) gene flow, the prospects for this phenomenon are
445 better, although predicated on receiving locations hosting healthy populations. Should
446 adaptive variants (such as conferring heat tolerance or bleaching resistance) exist in some
447 reefs then they might be able to spread naturally, with southward spread more probable. In
448 any event, increased knowledge regarding the directionality and magnitudes of genetic
449 exchange among GBR reefs will help forecast possible future evolutionary dynamics and can

450 help identify dispersal barriers that could be circumvented via assisted migration (Hoffmann
451 et al. 2015). In the case of GBR corals, assisted movements in a northward direction would
452 bypass natural dispersal limitations.
453
454 *Detecting contemporary asymmetric planktonic larval dispersal*
455 Relatively few studies have evaluated the effect of asymmetric larval dispersal on spatial
456 genetic patterns in marine species (Riginos et al., 2016). Perhaps not surprisingly, these
457 studies, like our results here with *A. tenuis* and *A. millepora,* consistently uncover substantial
458 asymmetries in inferred dispersal (e.g., Benestan et al., 2016; Dalongeville et al., 2018; Xuereb
459 et al., 2018). Clearly, conventional analyses, especially those based on summary statistics like
460 F_{ST} where all directional information is obscured, will fail to uncover important elements
461 regarding relationships among populations (Kool et al., 2013; Riginos et al., 2016).
462
463 An additional challenge is to clarify the time frame for processes yielding asymmetric spatial
464 genetic patterns. Empirical genomic data paired with specific historical demographic
465 simulations can sometimes put bounds on the timing and directionality of gene flow (as in
466 Duranton et al., 2018; Matz et al., 2018), but such approaches are largely constrained to
467 examining a few populations at a time due to exponential increase in number of potential free
468 parameters (for example, if migration is free to vary among n populations then there will be
469 n!/(n-2)! parameters for directional migration). Moreover, there is greater uncertainty
470 surrounding parameter estimation for recent events (Robinson, Coffman, Hickerson, &
471 Gutenkunst, 2014). Simple frequentist approaches based on linear models such as AEMs
472 represent an attractive alternative especially as they have been conceived for uncovering
473 contemporary structuring processes in species composition of ecological communities (Dray
474 et al., 2006), but if applied to intraspecific genetic data these approaches are likely to be
475 misleading when historical events have strongly shaped spatial genetic patterns.
476
477 In the present study, we attempted to bridge this historical-contemporary dilemma by using
478 constrained historical demographic simulations to reject the historical scenario most likely to
479 influence observable spatial genetic patterns for GBR species, giving us greater confidence
480 that the spatial genetic patterns we observe for *A. tenuis* and (to a lesser extent) *A. millepora*
481 reflect evolutionary processes from the recent past. Using prior information based on geology,
482 historical habitat shifts, or histories of co-distributed species to identify relevant alternative

483 hypotheses and then evaluating those hypotheses against hypotheses based on contemporary
484 gene flow (such as simple stepping-stone gene flow as used here) is a reasonable check of
485 data before proceeding to interpret results from linear models (including AEMs) at face value.
486
487 *Biophysical models as summaries of larval dispersal*
488 Biophysical models are increasingly being used to make detailed spatial predictions of
489 planktonic larval dispersal often with the aim of guiding management actions (as in Hock et
490 al., 2016; 2017; 2019; Krueck et al., 2017). Although such complex models of natural systems
491 cannot be truly tested (Oreskes et al., 1994), alignment of model outputs against independent
492 biological data can provide greater confidence that a biophysical larval dispersal model
493 captures elements of biological reality. In the present study, we find that directions and
494 relative magnitudes of dispersal connections derived from biophysical models are better
495 predictors of spatial genetic structure in *A. tenuis* and *A. millepora* than null models of
496 symmetric relationships, providing some confirmation that real biological processes mirror
497 expectations arising from biophysical simulations. The superior predictive power of
498 asymmetric predictors provides further evidence of the need to consider directional flow
499 when analysing connectivity in marine systems.
500
501 For our *Acropora* species on the GBR, the strongest alignments between the models and
502 empirical genetic data are at large spatial scales (among regions) and involve north to south
503 connections. Because small numbers of migrants can homogenize allele frequencies between
504 populations, inferences based on allele frequencies are poorly suited to distinguishing
505 strengths of demographically significant connections (Waples, 1998). Allele frequency based
506 methods, however, can theoretically discriminate between rare and very rare connections
507 such as those that are likely to link geographically distant populations (including via
508 multigenerational connections). Thus, the appropriate spatial scale for evaluating biophysical
509 larval dispersal models with population genetic data is at large spatial distances such a
510 regional connections among GBR coral populations where we find the greatest concordance
511 between predicted and observed patterns. Comprehensive evaluation of biophysical models
512 will best be undertaken with a variety of complementary empirical data types (Gaggiotti,
513 2017; Jones, 2015), where geographic patterns of allelic distributions contribute valuable
514 information about rare long-distance connections. Here we have shown that the directionality
515 of such rare long-distance connections discerned from spatial distributions of alleles provides

additional useful information for gauging concordance of larval dispersal models against past gene flow.

Acknowledgements:

We thank FG Blanchet for guidance on creating connexion diagrams and C Doropoulos for help with parameterisation of the dispersal models, the QRIS computing cluster for enabling simulation modelling, and funding support from the Great Barrier Reef Foundation.

Data accessibility statement: Raw data available at datadryad.org/resource/doi:10.5061/dryad.h8gh3 for *Acropora tenuis* and datadryad.org/resource/doi:10.5061/dryad.q0834p71 for *Acropora millepora.* Scripts, datafiles, and example results are available on GitHub: github.com/khock1/CoralPaths; github.com/dinmatias; github.com/CRiginos1.

REFERENCES

Abbey, E., Webster, J. M., & Beaman, R. J. (2011). Geomorphology of submerged reefs on the shelf edge of the Great Barrier Reef: The influence of oscillating Pleistocene sea-levels. *Marine Geology*, *288*(1-4), 61–78. http://doi.org/10.1016/j.margeo.2011.08.006

Anthony, K. R. N., Bay, L., Costanza, R., Firn, J., Gunn, J., Harrison, P., et al. (2017). New interventions are needed to save coral reefs. *Nature Ecology & Evolution*, *1*(10), 1–3. http://doi.org/10.1038/s41559-017-0313-5

Beger, M., Linke, S., Watts, M., Game, E., Treml, E. A., Ball, I., & Possingham, H. P. (2010). Incorporating asymmetric connectivity into spatial decision making for conservation. *Conservation Letters*, *3*(5), 359–368. http://doi.org/10.1111/j.1755-263X.2010.00123.x

Benestan, L., Quinn, B. K., Maaroufi, H., Laporte, M., Clark, F. K., Greenwood, S. J., et al. (2016). Seascape genomics provides evidence for thermal adaptation and current-mediated population structure in American lobster (*Homarus americanus*). *Molecular Ecology*, *25*(20), 5073–5092. http://doi.org/10.1111/mec.13811

Blanchet, F. G., Legendre, P., & Borcard, D. (2008). Modelling directional spatial processes in ecological data. *Ecological Modelling*, *215*(4), 325–336. http://doi.org/10.1016/j.ecolmodel.2008.04.001

Blanchet, F. G., Legendre, P., Maranger, R., Monti, D., & Pepin, P. (2011). Modelling the effect of directional spatial ecological processes at different scales. *Oecologia*, *166*(2), 357–368. http://doi.org/10.1007/s00442-010-1867-y

Borcard, D., & Legendre, P. (2002). All-scale spatial analysis of ecological data by means of principal coordinates of neighbour matrices. *Ecological Modelling*, *153*(1-2), 51–68. http://doi.org/10.1016/S0304-3800(01)00501-4

Boykov, Y., & Kolmogorov, V. (2004). An experimental comparison of min-cut/max- flow algorithms for energy minimization in vision. *IEEE Transactions on Pattern Analysis and Machine Intelligence*, *26*(9), 1124–1137. http://doi.org/10.1109/TPAMI.2004.60

Carr, M. H., Neigel, J., Estes, J., Andelman, S., Warner, R., & Largier, J. (2003). Comparing marine and terrestrial ecosystems: Implications for the design of coastal marine reserves. *Ecological Applications*, *13*(1), S90–S107.

Choukroun, S., Ridd, P. V., Brinkman, R., & McKinna, L. I. W. (2010). On the surface circulation in the western Coral Sea and residence times in the Great Barrier Reef. *Journal of Geophysical Research*, *115*(C6), 239. http://doi.org/10.1029/2009JC005761

Cowen, R. K., & Sponaugle, S. (2009). Larval dispersal and marine population connectivity. *Annual Review of Marine Science*, *1*(1), 443–466. http://doi.org/10.1146/annurev.marine.010908.163757

Crandall, E. D., Treml, E. A., & Barber, P. H. (2012). Coalescent and biophysical models of stepping-stone gene flow in neritid snails. *Molecular Ecology*, *21*(22), 5579–5598. http://doi.org/10.1111/mec.12031

Dalongeville, A., Andrello, M., Mouillot, D., Lobreaux, S., Fortin, M.-J., Lasram, F., et al. (2018). Geographic isolation and larval dispersal shape seascape genetic patterns differently according to spatial scale. *Evolutionary Applications*, *11*(8), 1437–1447. http://doi.org/10.1111/eva.12638

De'ath, G., Fabricius, K. E., Sweatman, H. P. A., & Puotinen, M. (2012). The 27-year decline of coral cover on the Great Barrier Reef and its causes. *Proceedings of the National Academy of Sciences of the United States of America*, *109*(44), 17995–17999. http://doi.org/10.1073/pnas.1208909109

Dijkstra, E. W. (1959). A note on two problems in connexion with graphs. *Numerische Mathematik*, *1*(1), 269–271. http://doi.org/10.1007/BF01386390

Diniz-Filho, J. A. F., Nabout, J. C., Telles, M. P. de C., Soares, T. N., & Rangel, T. F. L. V. B. (2009).

A review of techniques for spatial modeling in geographical, conservation and landscape genetics. *Genetics and Molecular Biology*, *32*(2), 203–211. http://doi.org/10.1590/S1415-47572009000200001

Dray, S., Legendre, P., & Peres-Neto, P. R. (2006). Spatial modelling: a comprehensive framework for principal coordinate analysis of neighbour matrices (PCNM). *Ecological Modelling*, *196*(3-4), 483–493. http://doi.org/10.1016/j.ecolmodel.2006.02.015

Duranton, M., Allal, F., Fraïsse, C., Bierne, N., Bonhomme, F., & Gagnaire, P.-A. (2018). The origin and remolding of genomic islands of differentiation in the European sea bass. *Nature Communications*, *9*(1), 1–11. http://doi.org/10.1038/s41467-018-04963-6

Excoffier, L., & Lischer, H. E. L. (2010). Arlequin suite ver 3.5: a new series of programs to perform population genetics analyses under Linux and Windows. *Molecular Ecology Resources*, *10*(3), 564–567. http://doi.org/10.1111/j.1755-0998.2010.02847.x

Excoffier, L., Dupanloup, I., Huerta-Sánchez, E., Sousa, V. C., & Foll, M. (2013). Robust demographic inference from genomic and SNP data. *PLoS Genetics*, *9*(10), e1003905. http://doi.org/10.1371/journal.pgen.1003905

Ford, L. R., & Fulkerson, D. R. (1956). Maximal flow through a network. *Canadian Journal of Mathematics*, *8*(0), 399–404. http://doi.org/10.4153/CJM-1956-045-5

Foster, N. L., Paris, C. B., Kool, J. T., Baums, I. B., Stevens, J. R., Sanchez, J. A., et al. (2012). Connectivity of Caribbean coral populations: complementary insights from empirical and modelled gene flow. *Molecular Ecology*, *21*(5), 1143–1157. http://doi.org/10.1111/j.1365-294X.2012.05455.x

Gaggiotti, O. E. (2017). Metapopulations of marine species with larval dispersal: a counterpoint to Ilkka's Glanville Fritillary metapopulations. *Annales Zoologici Fennici*, *54*(1-4), 97–112. http://doi.org/10.5735/086.054.0110

Gaines, S. D., White, C., Carr, M. H., & Palumbi, S. R. (2010). Designing marine reserve networks for both conservation and fisheries management. *Proceedings of the National Academy of Sciences of the United States of America*, *107*(43), 18286–18293. http://doi.org/10.1073/pnas.0906473107

Galindo, H. M., Olson, M. V., & Palumbi, S. R. (2006). Seascape genetics: A coupled oceanographic-genetic model predicts population structure of Caribbean corals. *Current Biology*, *16*(16), 1622–1626. http://doi.org/10.1016/j.cub.2006.06.052

GBRMPA. Great Barrier Reef Marine Park Zoning Plan 2003. Report No. ISBN9781876945237, 1-211 (Great Barrier Reef Marine Park Authority, Townsville, QLD, Australia, 2004).

Hellberg, M. E. (2009). Gene flow and isolation among populations of marine animals. *Annual Review of Ecology, Evolution, and Systematics*, *40*(1), 291–310. http://doi.org/10.1146/annurev.ecolsys.110308.120223

Hinestrosa, G., Webster, J. M., & Beaman, R. J. (2016). Postglacial sediment deposition along a mixed carbonate-siliciclastic margin: New constraints from the drowned shelf-edge reefs of the Great Barrier Reef, Australia. *Palaeogeography, Palaeoclimatology, Palaeoecology*, *446*, 168–185. http://doi.org/10.1016/j.palaeo.2016.01.023

Hock, K., Doropoulos, C., Gorton, R., Condie, S.A., & Mumby, P.J. (2019) Split spawning increases robustness of coral larval supply and inter-reef connectivity. *Nature Communications. In press.*

Hock, K., & Mumby, P. J. (2015). Quantifying the reliability of dispersal paths in connectivity networks. *Journal of the Royal Society Interface*, *12*(105), 20150013–20150013. http://doi.org/10.1098/rsif.2015.0013

Hock, K., Wolff, N. H., Beeden, R., Hoey, J., Condie, S. A., Anthony, K. R. N., et al. (2016). Controlling range expansion in habitat networks by adaptively targeting source populations. *Conservation Biology*, *30*(4), 856–866. http://doi.org/10.1111/cobi.12665

Hock, K., Wolff, N. H., Ortiz, J. C., Condie, S. A., Anthony, K. R. N., Blackwell, P. G., & Mumby, P. J. (2017). Connectivity and systemic resilience of the Great Barrier Reef. *PLoS Biology*, *15*(11), e2003355–23. http://doi.org/10.1371/journal.pbio.2003355

Hoffmann, A. A., Griffin, P. C., Dillon, S., Catullo, R. A., Rane, R., Byrne, M., et al. (2015). A framework for incorporating evolutionary genomics into biodiversity conservation and management. *Climate Change Responses*, *2*(1), 1–24. http://doi.org/10.1186/s40665-014-0009-x

Hughes, T. P., Kerry, J. T., Álvarez-Noriega, M., Álvarez-Romero, J. G., Anderson, K. D., Baird, A. H., et al. (2017). Global warming and recurrent mass bleaching of corals. *Nature*, *543*(7645), 373–377. http://doi.org/10.1038/nature21707

Hughes, T. P., Kerry, J. T., Baird, A. H., Connolly, S. R., Dietzel, A., Eakin, C. M., et al. (2018). Global warming transforms coral reef assemblages. *Nature*, *556*(7702), 492–496. http://doi.org/10.1038/s41586-018-0041-2

Johnson, M. S., Black, R. 1984. Pattern beneath the chaos: the effect of recruitment on genetic patchiness in an intertidal limpet. *Evolution* 38: 1371-1383.

Jones, G. P. (2015). Mission impossible: unlocking the secrets of coral reef fish dispersal. In C. Mora (Ed.), *Ecology of Fishes on Coral Reefs* (pp. 16–27). Cambridge: Cambridge University Press. http://doi.org/10.1017/cbo9781316105412.004

Kool, J. T., Moilanen, A., & Treml, E. A. (2013). Population connectivity: recent advances and new perspectives. *Landscape Ecology*, *28*(2), 165–185. http://doi.org/10.1007/s10980-012-9819-z

Kool, J. T., Paris, C. B., Andréfouët, S., & Cowen, R. K. (2010). Complex migration and the development of genetic structure in subdivided populations: an example from Caribbean coral reef ecosystems. *Ecography*, *105*, 26191–10. http://doi.org/10.1111/j.1600-0587.2009.06012.x

Kool, J. T., Paris, C. B., Barber, P. H., & Cowen, R. K. (2011). Connectivity and the development of population genetic structure in Indo-West Pacific coral reef communities. *Global Ecology and Biogeography*, *20*(5), 695–706. http://doi.org/10.1111/j.1466-8238.2010.00637.x

Kritzer, J. P., & Sale, P. F. (2004). Metapopulation ecology in the sea: from Levins' model to marine ecology and fisheries science. *Fish and Fisheries*, *5*(2), 131–140. http://doi.org/10.1111/j.1467-2979.2004.00131.x

Krueck, N. C., Ahmadia, G. N., Green, A., Jones, G. P., Possingham, H. P., Riginos, C., et al. (2017). Incorporating larval dispersal into MPA design for both conservation and fisheries. *Ecological Applications 27*(3), 925–941. http://doi.org/10.1002/eap.1495

Legendre, P., & Gallagher, E. D. (2001). Ecologically meaningful transformations for ordination of species data. *Oecologia*, *129*(2), 271–280. http://doi.org/10.1007/s004420100716

Liggins, L., Treml, E. A., & Riginos, C. (2013). Taking the plunge: an introduction to undertaking seascape genetic studies and using biophysical models. *Geography Compass*, *7*(3), 173–196. http://doi.org/10.1111/gec3.12031

Lukoschek, V., Cross, P., Torda, G., Zimmerman, R., & Willis, B. L. (2013). The importance of coral larval recruitment for the recovery of reefs impacted by Cyclone Yasi in the central Great Barrier Reef. *PloS ONE*, *8*(6), e65363–11. http://doi.org/10.1371/journal.pone.0065363

Lukoschek, V., Riginos, C., & van Oppen, M. J. H. (2016). Congruent patterns of connectivity can inform management for broadcast spawning corals on the Great Barrier Reef. *Molecular Ecology*, *25*(13), 3065–3080. http://doi.org/10.1111/mec.13649

Mao, Y., & Luick, J. L. (2014). Circulation in the southern Great Barrier Reef studied through an integration of multiple remote sensing and in situ measurements. *Journal of Geophysical*

Research: Oceans, *119*(3), 1621–1643. http://doi.org/10.1002/2013JC009397
Marshall, D. J., Monro, K., Bode, M., Keough, M. J., & Swearer, S. (2010). Phenotype-environment mismatches reduce connectivity in the sea. *Ecology Letters*, *13*(1), 128–140. http://doi.org/10.1111/j.1461-0248.2009.01408.x
Matz, M. V., Treml, E. A., Aglyamova, G. V., & Bay, L. (2018). Potential and limits for rapid genetic adaptation to warming in a Great Barrier Reef coral. *PLoS Genetics*, *14*(4), e1007220–19. http://doi.org/10.1371/journal.pgen.1007220
Metaxas, A., & Saunders, M. (2009). Quantifying the "bio-" components in biophysical models of larval transport in marine benthic invertebrates: advances and pitfalls. *The Biological Bulletin*, *216*(3), 257–272. http://doi.org/10.1086/BBLv216n3p257
Oreskes, N., Shrader-Frechette, K., & Belitz, K. (1994). Verification, validation, and confirmation of numerical models in the Earth sciences. *Science*, *263*(5147), 641–646. http://doi.org/10.1126/science.263.5147.641
Pineda, J., Hare, J. A., & Sponaugle, S. (2007). Larval transport and dispersal in the coastal ocean and consequences for population connectivity. *Oceanography*, *20*(3), 22–39.
Planes, S., & Doherty, P. J. (1997). Genetic and color interactions at a contact zone of *Acanthochromis polyacanthus*: a marine fish lacking pelagic larvae. *Evolution*, *51*(4), 1232–1243. http://doi.org/10.1111/j.1558-5646.1997.tb03970.x
Pratchett, M. S., Caballes, C. F., Rivera-Posada, J. A., & Sweatman, H. P. A. (2014). Limits to understanding and managing outbreaks of crown-of-thorns starfish (*Acanthaster spp*.). *Oceanography and Marine Biology*, 1–68.
Pringle, J. M., & Wares, J. P. (2007). Going against the flow: maintenance of alongshore variation in allele frequency in a coastal ocean. *Marine Ecology Progress Series*, *335*, 69–84. http://doi.org/10.3354/meps335069
Riginos, C., & Liggins, L. (2013). Seascape genetics: populations, individuals, and genes marooned and adrift. *Geography Compass 7*(3), 197–216. http://doi.org/10.1111/gec3.12032
Riginos, C., Crandall, E. D., Liggins, L., Bongaerts, P., & Treml, E. A. (2016). Navigating the currents of seascape genomics: how spatial analyses can augment population genomic studies. *Current Zoology*, *62*(6), 581–601. http://doi.org/10.1093/cz/zow067
Robinson, J. D., Coffman, A. J., Hickerson, M. J., & Gutenkunst, R. N. (2014). Sampling strategies for frequency spectrum-based population genomic inference. *BMC Evolutionary Biology*, *14*(1), 254. http://doi.org/10.1186/s12862-014-0254-4
Roux, C., Fraïsse, C., Romiguier, J., Anciaux, Y., Galtier, N., & Bierne, N. (2016). Shedding light on the grey zone of speciation along a continuum of genomic divergence. *PLoS Biology*, *14*(12), e2000234–22. http://doi.org/10.1371/journal.pbio.2000234
Schunter, C., Carreras-Carbonell, J., Macpherson, E., Tintoré, J., Vidal-Vijande, E., Pascual, A., et al. (2011). Matching genetics with oceanography: directional gene flow in a Mediterranean fish species. *Molecular Ecology*, *20*(24), 5167–5181. http://doi.org/10.1111/j.1365-294X.2011.05355.x
Selkoe, K. A., D'Aloia, C. C., Crandall, E. D., Iacchei, M., Liggins, L., Puritz, J. B., et al. (2016a). A decade of seascape genetics: contributions to basic and applied marine connectivity. *Marine Ecology Progress Series*, *554*, 1–19. http://doi.org/10.3354/meps11792
Selkoe, K. A., Scribner, K. T., & Galindo, H. M. (2016b). Waterscape genetics – applications of landscape genetics to rivers, lakes, and seas. In N. Balkenhol, S. A. Cushman, A. Storfer, & L. P. Waits (Eds.), *Landscape Genetics: Concepts, Methods, Applications* (pp. 1–27). John Wiley & Sons, Ltd.
Sundqvist, L., Keenan, K., Zackrisson, M., Prodöhl, P., & Kleinhans, D. (2016). Directional genetic differentiation and relative migration. *Ecology and Evolution*, *6*(11), 3461–3475.

http://doi.org/10.1002/ece3.2096
Thomas, L., Kennington, W. J., Stat, M., Wilkinson, S. P., Kool, J. T., & Kendrick, G. A. (2015). Isolation by resistance across a complex coral reef seascape. *Proceedings of the Royal Society: Biological Sciences 282*(1812), 20151217. http://doi.org/10.1098/rspb.2015.1217
Truelove, N. K., Kough, A. S., Behringer, D. C., Paris, C. B., Box, S. J., Preziosi, R. F., & Butler, M. J. (2016). Biophysical connectivity explains population genetic structure in a highly dispersive marine species. *Coral Reefs*, 1–13. http://doi.org/10.1007/s00338-016-1516-y
van Oppen, M. J. H., Peplow, L. M., Kinnimonth, S., & Berkelmans, R. (2011). Historical and contemporary factors shape the population genetic structure of the broadcast spawning coral, *Acropora millepora*, on the Great Barrier Reef. *Molecular Ecology*, *20*(23), 4899–4914. http://doi.org/10.1111/j.1365-294X.2011.05328.x
Waples, R. S. (1998). Separating the wheat from the chaff: patterns of genetic differentiation in high gene flow species. *The Journal of Heredity*, *89*(5), 438–450. http://doi.org/10.1093/jhered/89.5.438
Watson, J. R., Kendall, B. E., Seigel, D. A., & Mitarai, S. (2012). Changing seascapes, stochastic connectivity, and marine metapopulation dynamics. *American Naturalist*, *180*(1), 99–112. http://doi.org/10.1086/665992
Werner, F., & Cowen, R. K. (2007). Coupled biological and physical models: present capabilities and necessary developments for future studies of population connectivity. *Oceanography*, *20*, 54–69.
White, C., Selkoe, K. A., Watson, J., Siegel, D. A., Zacherl, D. C., & Toonen, R. J. (2010). Ocean currents help explain population genetic structure. *Proceedings. Biological Sciences / the Royal Society*, *277*(1688), 1685–1694. http://doi.org/10.1098/rspb.2009.2214
Whitlock, M. C., & McCauley, D. E. (1999). Indirect measures of gene flow and migration: FST not equal to 1/(4Nm + 1). *Heredity*, *82*, 117–125. Retrieved from http://eutils.ncbi.nlm.nih.gov/entrez/eutils/elink.fcgi?dbfrom=pubmed&id=10098262&retmode=ref&cmd=prlinks
Wolff, N. H., Mumby, P. J., Devlin, M., & Anthony, K. R. N. (2018). Vulnerability of the Great Barrier Reef to climate change and local pressures. *Global Change Biology*, *24*(5), 1978–1991. http://doi.org/10.1111/gcb.14043
Xuereb, A., Benestan, L., Normandeau, E., Curtis, J. M., Bernatchez, L., & Fortin, M.-J. (2018). Asymmetric oceanographic processes mediate connectivity and population genetic structure, as revealed by RADseq, in a highly dispersive marine invertebrate (*Parastichopus californicus*). *Molecular Ecology*, 1–46.

Biosketch: The authors are linked by a desire to better understand how planktonic larval dispersal connects marine populations. Advances in measuring and predicting dispersal connections are urgently needed in the context of the Great Barrier Reef where there have been recent widespread outbreaks of coral bleaching. Thus, progress in uncovering the dynamics of long-distance dispersal connections contributes to an ultimate goal of identifying locations best-able to supply propagules and seed downstream reefs. Author contributions: CR and VL conceived the overarching concept and KH, AMM, PJM, & MJHvO contributed ideas fundamental to the study; VL, MJHvO, and KH collected the data; CR, KH, and AMM analysed the data and developed the figures; and CR led the writing with contributions from KH, AMM, PJM, MJHvO & VL.

773 **TABLES**

774

775 **Table 1:** Spatial eigenvector map modelling of genetic structure. The models explaining the greatest amount of genetic variance are
776 those that incorporate directional link structures derived from the larval dispersal model, especially those that are based on north to
777 south alongshore flow.

		Acropora tenuis			*Acropora millepora*		
Eigenmodel	**Link structure**	**Link weighting of best model** [a]	**Numb EMs in best model** [b]	**adjusted R^2** [b]	**Link weighting of best model** [a]	**Numb EMs in best model** [b]	**adjusted R^2** [b]
MEM	Delaunay	Binary	1	0.02	Binary	1	0.02
MEM	Delaunay	log	1	0.03	log	1	0.03
MEM	PCNM	y=1	**4**	**0.24***	log	**1**	**0.09**
MEM	Custom saturated	y=1	3	0.16*	log	1	0.10
AEM	Alongshore N to S only [c]	MF, y=1	**9**	**0.37**	Binary	**5**	**0.27**
AEM	Alongshore both N to S and S to N	SS, y=1	8	0.29	MF, y=1	2	0.15

778

779 [a] Binary distances represent a single model. The link structures were evaluated for link distance weightings based on the formula 1-
780 $(D/Dmax)^y$ for y=[1-3] or with a log transformation to approximate a typical isolation-by-distance analysis. For AEMs, links were limited
781 to those in the top 50 percentile of reliable path weights. Link weightings were evaluated based on the number of stepping stone (SS)
782 connections, maximum flow (MF), and reliable path (RP) strength.

783 [b] Following forward model selection; asterisks indicate spatial models with **Δ**AICc < 2 as compared to the null (intercept only) model.

784 [c] Select AEMs shown graphically in Fig. 4 and Sup. Fig. 3

785

Table 2: Asymmetric eigenvector map modelling regions within *Acropora tenuis*

	Best model by region			
Region	**Link structure**	**Link weighting** [a]	**Numb EMs in best model** [b]	**adjusted R^2** [b]
Far north & north	Alongshore both N to S and S to N	MF, y=1	**3**	0.17
North, central, south	Alongshore N to S	MF, y=1	**7**	0.32
Central & south	Alongshore N to S	RP, y=2	**5**	0.35

[a] Link structures were evaluated for distance weightings based on the formula $1-(D/Dmax)^y$ for y=[1-3].

[b] Following forward model selection.

790 **FIGURE LEGENDS**

791 **Figure 1:** Sampling locations and main attributes of biophysical model. A) Coastal Queensland
792 and the Great Barrier Reef where bathymetry is shown by grey shading and 120 m depth
793 reflects the approximate land mass exposure at lowest Pleistocene sea level stands.
794 Designated regions correspond to management areas. Major offshore currents are shown
795 (NVJ and SVJ: north and south Vanuatu jets, NQC: north Queensland current, EAC: east
796 Australia current; modified from Coukroun *et al.* 2010; Mao & Luick 2014). B & C) Summary of
797 top 50 percentile predicted connections based on relative path probabilities for *Acropora*
798 *tenuis* (B) and *Acropora millepora* (C). Sampling locations are color coded by latitude with
799 northern low latitude sites shown in reds (warm) and southern higher latitude sites shown in
800 blues (cool). Vectors show predicted dispersal probabilities with thicker lines indicating
801 higher probabilities and colored by source population. D & E) Dispersal probabilities relative
802 to coastline position for *Acropora tenuis* (D) and *Acropora millepora* (E). The largest positional
803 changes northwards have the lowest probabilities whereas small positional changes and
804 movements southwards have higher probabilities. Movement relative to coastline is based on
805 the difference in relative position between locations as summarised by the first principal
806 component axis describing Queensland coastline. Example contrasts in northward vs.
807 southward dispersal strengths shown for example population pairs (a,b and c,d) traversing
808 the length of the sampling region where a->b and c->d are high probabilities ($P \approx 10^{-20}$) of
809 southward movement (-4 relative positional change) and b->a and d->c are low probabilities
810 ($P \approx 10^{-40}$) of northward movement (+4 relative positional change).

811

812 **Figure 2:** Competing models of historical scenarios evaluated using Approximate Bayesian
813 Computation based on historical divergence vs. gene flow between adjacent stepping stone
814 populations. A) Representative populations chosen for comparison via ABC against simulated
815 data. B) Historical divergence models with a barrier to gene flow at Hydrographer's Passage.
816 C) Stepping-stone gene flow models where migration was permitted only between adjacent
817 populations but with rates free to vary. The prior distributions of the parameters are
818 summarized in Table S1. ABC analyses provided higher support for the stepping-stone gene
819 flow models (*A. tenuis*: posterior probability = 0.999; Bayes Factor = 1210; *A. millepora*: PP =
820 0.647; BF = 3) compared to the model of historical divergence vicariance.

821

822 **Figure 3:** Concordance in directional movement between the larval dispersal model and
823 genetic estimates for pairs of populations for *Acropora tenuis* (A), and *Acropora millepora* (B).
824 Routes of low predicted connectivity (small relative path probabilities: $P < 10^{-40}$) experience
825 low directional gene flow (using the DivMigrate method). Routes of high predicted
826 connectivity ($P > 10^{-20}$) have variable rates of gene flow.
827
828 **Figure 4:** Leading asymmetric eigenvector maps describing spatial genetic structure in
829 *Acropora tenuis*. Values by sampling location are colored by intensity of green hue such that
830 locations with similar colors have similar AEM values. The greatest proportion of variance
831 (AEM 1) describes a GBR-wide cline in genetic diversity followed by local scale spatial
832 autocorrelation structures (AEM 5).

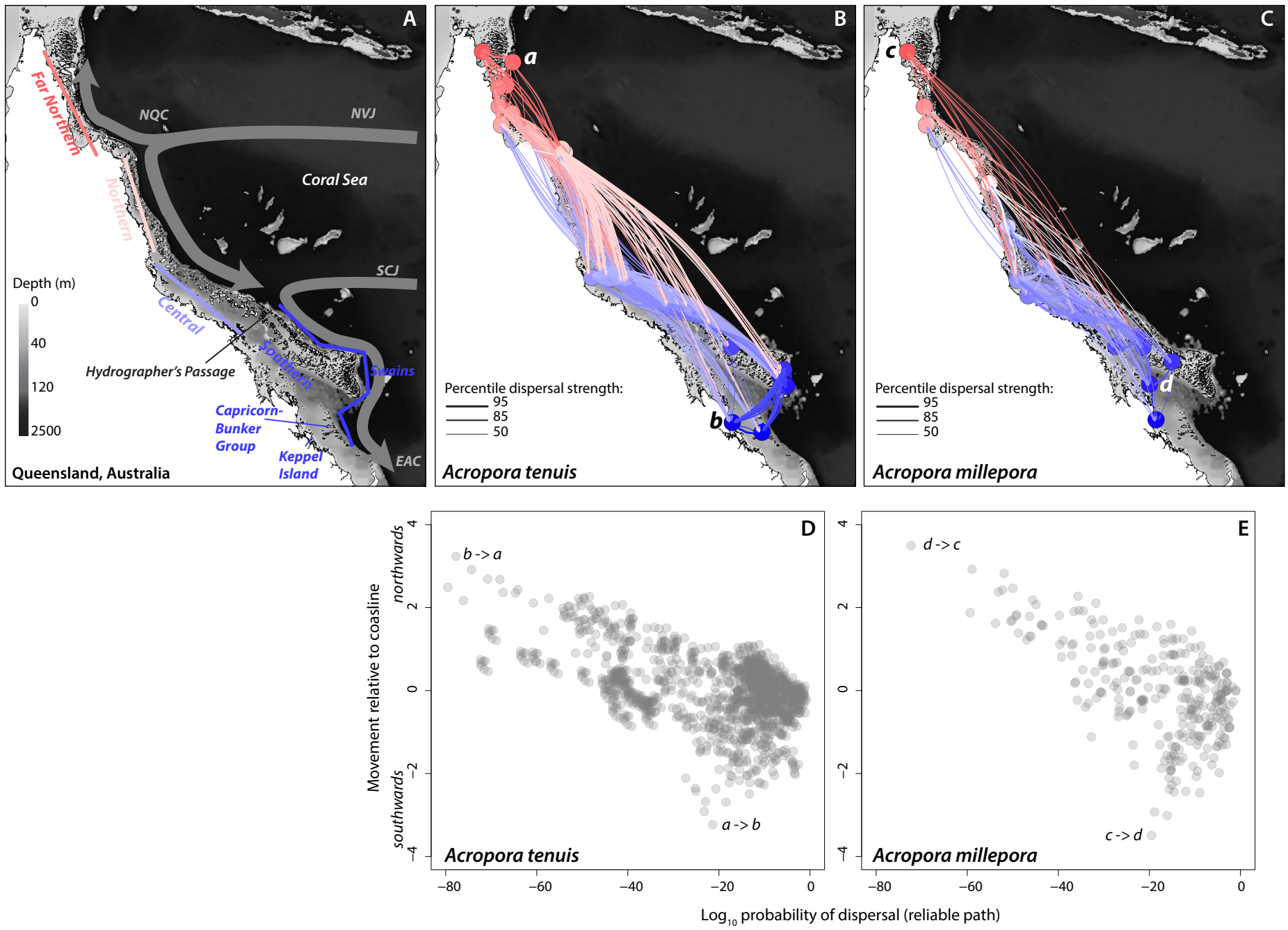
A
Far Northern
Northern
Central
Southern
Swains
NQC
NVJ
Coral Sea
SCJ
EAC
Depth (m)
0
40
120
2500
Hydrographer's Passage
Capricorn-Bunker Group
Keppel Island
Queensland, Australia
B
a
b
Percentile dispersal strength:
95
85
50
Acropora tenuis
C
c
d
Percentile dispersal strength:
95
85
50
Acropora millepora
D
b -> a
a -> b
Acropora tenuis
E
d -> c
c -> d
Acropora millepora
Movement relative to coasline
northwards
southwards
4
2
0
−2
−4
−80
−60
−40
−20
0
Log10 probability of dispersal (reliable path)

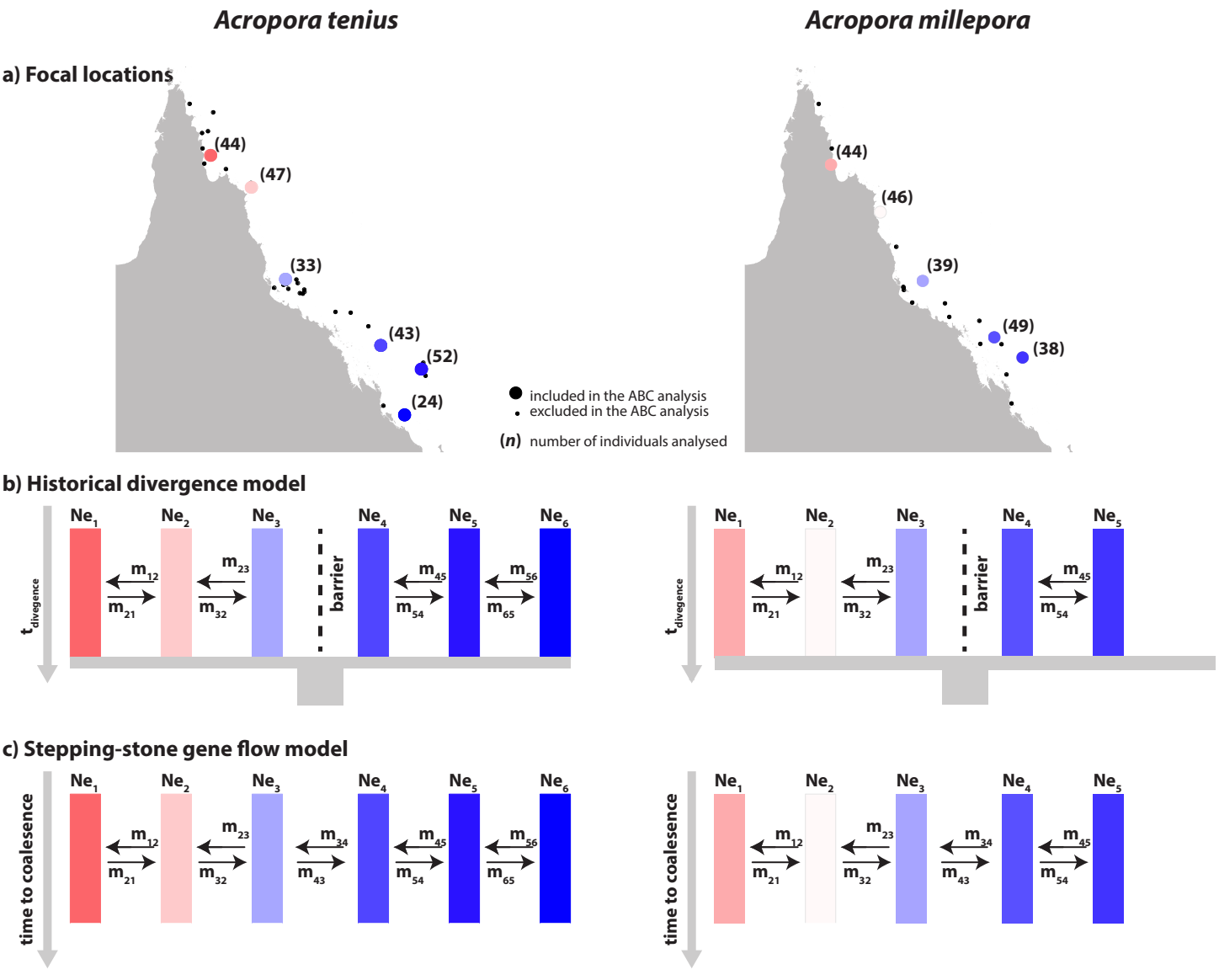
Acropora tenius
Acropora millepora
a) Focal locations
(44)
(47)
(33)
(43)
(52)
(24)
(44)
(46)
(39)
(49)
(38)
included in the ABC analysis
excluded in the ABC analysis
(n) number of individuals analysed
b) Historical divergence model
Ne1
Ne2
Ne3
Ne4
Ne5
Ne6
m12
m21
m23
m32
m45
m54
m56
m65
barrier
tdivegence
c) Stepping-stone gene flow model
m34
m43
time to coalesence

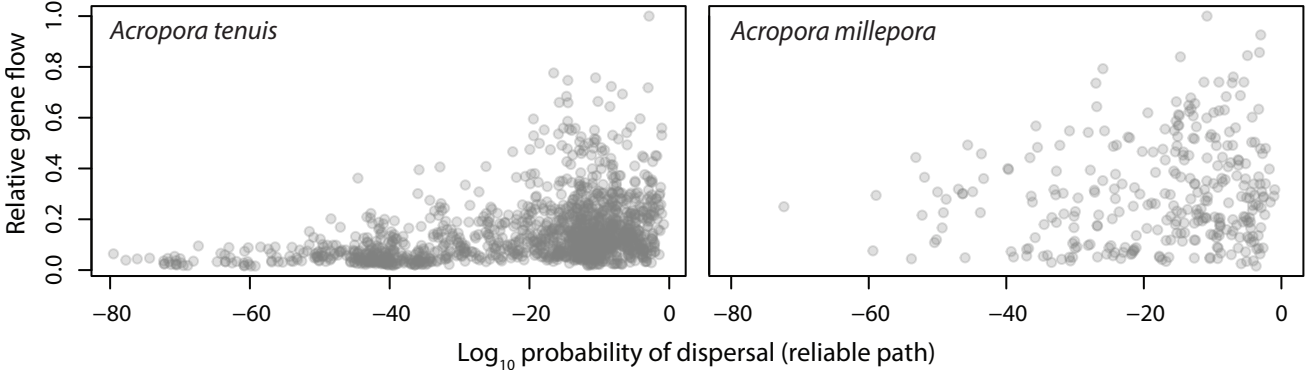
Acropora tenuis
Acropora millepora
Relative gene flow
0.0
0.2
0.4
0.6
0.8
1.0
−80
−60
−40
−20
0
Log10 probability of dispersal (reliable path)

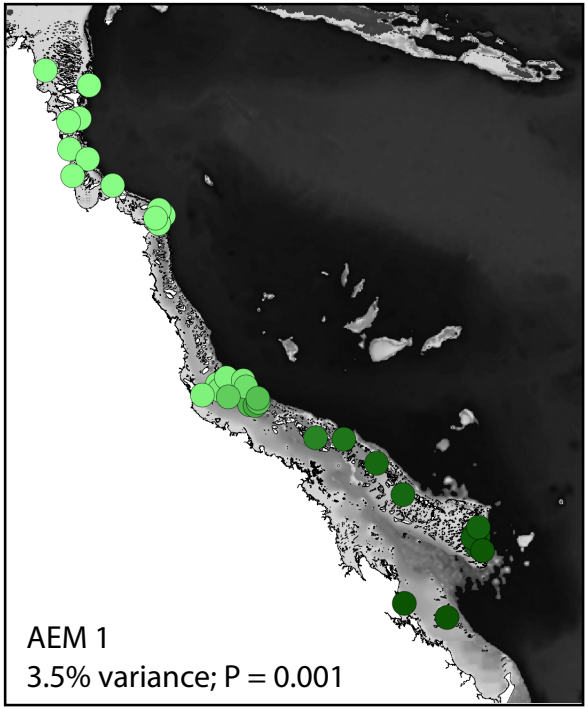
AEM 1
3.5% variance; P = 0.001

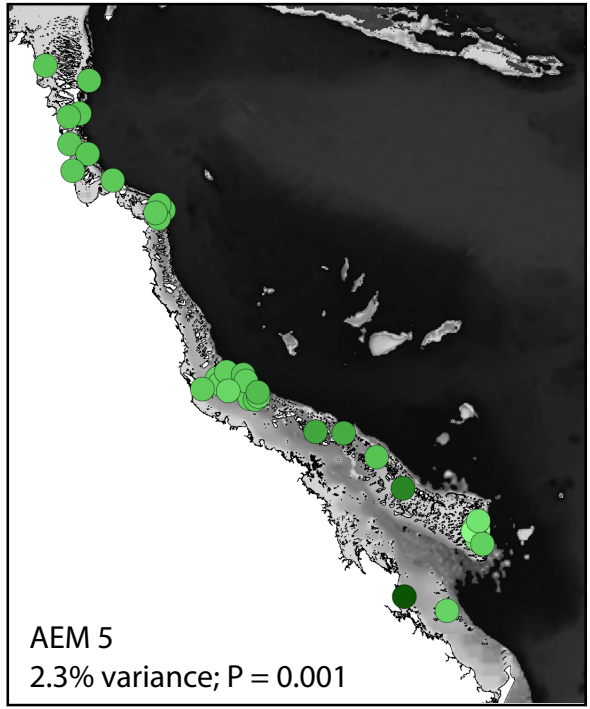
AEM 5
2.3% variance; P = 0.001